Acta Pharmacologica Sinica 2017: 1369–1380
 1671-4083/17
www.nature.com/aps

Original Article

Wenshen Zhuanggu formula effectively suppresses breast cancer bone metastases in a mouse xenograft model

Jia-jia LI[1, #], Wei-ling CHEN[1, #], Jian-yi WANG[2], Qian-wen HU[1], Zhen-ping SUN[1], Shuai ZHANG[1], Sheng LIU[1, *], Xiang-hui HAN[1, *]

[1]Institute of Chinese Traditional Surgery, Longhua Hospital Affiliated to Shanghai University of Traditional Chinese Medicine, Shanghai 200032, China; [2]Department of Liver Disease, Shuguang Hospital Affiliated to Shanghai University of Traditional Chinese Medicine, Shanghai 201203, China

Abstract

Wenshen Zhuanggu formula (WSZG) is a traditional Chinese medicine used as an adjuvant for the prevention of bone metastases in breast cancer patients. In this study we investigated the efficacy of WSZG in preventing bone metastases and the potential mechanisms in a mouse xenograft model of breast cancer bone metastases. This model was established by injection of human MDA-MB-231BO-Luc breast cancer cells alone or a mixture of the cancer cells with bone marrow-derived mesenchymal stem cells (BMSCs) into left ventricle of the heart in female nude mice. Then the mice were treated with WSZG (3.25, 6.5 or 13.0 $mg \cdot kg^{-1} \cdot d^{-1}$, ig) for four weeks, whereas zoledronic acid (100 μg/kg per week, ig) was used as a positive control. The occurrence and development of bone metastases were monitored via bioluminescent imaging, and bone lesions were assessed using micro-CT. Intracardiac injection of the mixture of MDA-MB-231BO-Luc breast cancer cells with BMSCs significantly facilitated the bone metastatic capacity of the breast cancer cells, and aggravated bone lesions in the mouse xenograft model of breast cancer bone metastases. Administration of WSZG dose-dependently inhibited the incidence and intensity of bone metastases and protected against bone lesions by suppressing osteoclast formation and tumor cell infiltration. Furthermore, administration of WSZG caused a marked reduction in the expression of CCL5/CCR5 and IL-17B/IL-17BR in bone metastatic tissues. The results demonstrate that WSZG exerts potential therapeutic effects in a mouse xenograft model of breast cancer bone metastases, which are partially mediated by weakening the interaction between BMSCs and breast cancer cells in the tumor microenvironment.

Keywords: breast cancer; bone metastases; traditional Chinese medicine; Wenshen Zhuanggu formula; zoledronic acid; bone marrow-derived mesenchymal stem cells; CCL5/CCR5; IL-17B/IL-17BR

Acta Pharmacologica Sinica (2017) 38: 1369–1380; doi: 10.1038/aps.2017.13; published online 17 Apr 2017

Introduction

The incidence of breast cancer among women has rapidly increased worldwide. Breast cancer cells spread from the primary site to distant organs, such as bones, lungs, and liver[1]. Bones are the most common sites of breast cancer metastases. Approximately 65% to 75% of advanced breast cancer patients eventually develop bone metastases, which remain the leading cause of death and have a five-year survival rate of only 20%[2]. Bone metastases are a major clinical concern and can cause pain, pathologic fractures, hypercalcemia, spinal cord compression, and other bone-related events. Bone metastases severely affect the life quality of patients. Routine treatments for breast cancer with bone metastases include radiotherapy, chemotherapy, and bisphosphonates. These therapies effectively reduce the frequency of bone-related events, inhibit cancer-mediated bone resorption, and reduce pain in bone-metastatic breast cancer patients[3]. However, these therapies have significant side effects, such as induction of arthralgias and osteonecrosis of the jaw. In China, the combination of modern western therapies and traditional Chinese medicine (TCM) is a common approach to treat breast cancer with bone metastases. As an important complementary therapy, Chinese herbal medicine can effectively resolve breast lumps, alleviate bone pain, minimize the adverse events of chemotherapy, and improve the overall health and well-being of cancer patients[4].

[#] These authors contributed equally to this work.
[*] To whom correspondence should be addressed.
E-mail hanxianghui1106@163.com (Xiang-hui HAN);
lshtcm@163.com (Sheng LIU)
Received 2016-11-08 Accepted 2017-02-27

The Wenshen Zhuanggu formula (WSZG), a TCM prescription, has been used extensively as an adjuvant to treat patients with breast cancer bone metastases in Longhua Hospital. WSZG is composed of the herbs *Fructus psoraleae* (Bu-Gu-Zhi in Chinese; Psoralea fruit, *Psoralea corylifolia* L), *Fructus cnidii* (She-Chuang-Zi in Chinese; Cnidium fruit, *Cnidium monnieri* L), and *Aconiti lateralis radix praeparata* (Fu-Zi in Chinese; processed aconite root, *Aconitum carmichaelii* Debx). A retrospective cohort study on 48 patients with breast cancer bone metastases confirmed that WSZG could prevent the development of bone metastases and improve the quality of life of the patients[5]. In a previous experimental study, WSZG significantly reduced the frequency of bone metastases and mitigated osteolytic lesions in nude mice with breast cancer bone metastases[6].

The underlying cellular and molecular mechanisms of breast cancer bone metastases remain complicated and unclear. Recently, increasing focus has been directed to the contribution of bone marrow-derived mesenchymal stem cells (BMSCs). As adult progenitor cells, BMSCs can differentiate into adipocytes, osteocytes, and chondrocytes under special conditions and promote stromal tissue renewal[7]. Many studies have affirmed that BMSCs are actively involved in breast carcinoma bone metastatic processes. On the one hand, BMSCs in the bone marrow facilitate the multiplication and morphology of breast cancer cells in the bone through paracrine factors and the secretion of chemotactic cytokines[8]. On the other hand, BMSCs in the circulating blood are recruited to the site of *in situ* breast tumor and stimulate the growth of tumors and the frequency of bone metastasis *via* the interaction between BMSCs and breast cancer cells[9].

In our previous study, we found that WSZG-containing serum exerts an anti-metastatic activity against MDA-MB-231BO breast cancer cells by preventing the interaction between BMSCs and breast cancer cells *in vitro*[10]. Therefore, in the present study, we further explored the pharmacological activities and potential mechanisms of WSZG in an animal model of breast cancer bone metastases.

Materials and methods

Plant materials and preparation of WSZG

Fructus psoraleae, *Fructus cnidii*, and *Aconiti lateralis radix praeparata* were purchased from Shanghai Kang Qiao Chinese Cut Crude Drug Co Ltd (Shanghai, China, Lot 12615) and authenticated by Prof Zhi-li ZHAO from the Department of Pharmacognosy, Shanghai University of TCM. Morphological, microscopic, and phytochemical identifications were performed according to the Pharmacopoeia of the People's Republic of China (2010 edition). Herbarium voucher specimens were deposited at Longhua Hospital, which is affiliated with Shanghai University of TCM, with voucher numbers as follows: BGZ-1207081 for *Fructus psoraleae*, SCZ-1207082 for *Fructus cnidii*, and FZ-1207083 for *Aconiti lateralis radix praeparata*.

A WSZG extract was prepared according to our previous method[10]. Briefly, *Fructus psoraleae*, *Fructus cnidii*, and *Aconiti lateralis radix praeparata* were mixed at a ratio of 5:5:3. The mixture was immersed in 55% ethanol (1:10, *w/v*) for 4 h and refluxed for 1.5 h. After filtration, the residue was refluxed again with 55% ethanol (1:8, *w/v*) for 1 h and filtered. Thereafter, the two decoctions were combined and concentrated with a vacuum to a final concentration of 2 g/mL. The ethanol in the extract was volatilized completely. Quality assurance for the WSZG extract was carried out by quantifying three marker compounds with high-performance liquid chromatography (HPLC). The results of HPLC analysis were the same as described in our previous *in vitro* experiment. The content of psoralen, isopsoralen, and osthole in the extract was 15.3, 11.6, and 25.2 mg/g, respectively[10].

Chemicals and reagents

Rabbit polyclonal antibodies, namely, anti-CCL5, anti-CCR5, anti-IL-17B, and anti-IL-17BR, were purchased from Abcam Trading (Shanghai) Company Ltd (Shanghai, China). Rabbit anti-goat secondary antibodies were obtained from Jackson Immuno Research Laboratories Inc (West Grove, PA, USA). EnVision/HRP kits were acquired from Dako Cytomation, Denmark. PrimeScript® RT reagent kits and SYBR Premix Ex Taq™ kits were obtained from TaKaRa Biotechnology (Dalian) Co, Ltd (Dalian, China). *D*-luciferin potassium was acquired from Cellcyto Co, Ltd (Shanghai, China). All other chemicals used were of analytical grade and were obtained from Sigma (St Louis, MO, USA).

Cell culture

Human fetal BMSCs (Cat No HUXMF-01001) were obtained from Cyagen Bioscience (Guangzhou) Inc (Guangzhou, China). These BMSCs are positive for CD29, CD44, and CD105 but negative for CD34 and CD45. Human breast cancer MDA-MB-231BO cells were donated by Dr Toshiyuki YONEDA (Osaka University). These cells stably express the firefly luciferase (Luc) reporter gene. Both cells were cultured in Dulbecco's modified Eagle's medium (DMEM) supplemented with 10% fetal bovine serum, 100 IU/mL of penicillin, 100 μg/mL of streptomycin, and 1% *L*-glutamine in a humidified atmosphere of 5% CO_2 and 95% air at 37 °C.

Animals

Female athymic nude mice (BALB/c, 6–8 weeks, weighing 18.0±1.3 g) were obtained from Shanghai Experimental Animal Center of Chinese Academy of Sciences and housed in a 12 h dark/light cycle environment at a temperature of 22±2 °C and relative air humidity of 45%–55%. Food and water were provided *ad libitum*. All animals received humane care in strict accordance with the recommendations in the Guide for the Care and Use of Laboratory Animals of the National Institutes of Health. The protocol was approved by the Animal Research Ethics Committee of Shanghai University of TCM (Permit Number: 12010). All surgeries were performed under sodium pentobarbital anesthesia, and all efforts were exerted

to minimize suffering.

Xenograft model of breast cancer bone metastases and drug treatment

A xenograft model of bone metastases was established as previously described[11]. Briefly, after anaesthetization with 75 mg/kg of pentobarbital sodium, the mice were injected with Luc-labeled cancer cells alone (0.5×10^6 cells per mouse, suspended in 100 μL of phosphate-buffered saline) or mixed with BMSCs (0.5×10^6 cells per mouse, 1:1 mixture) into the left ventricle of the heart. The development and growth of bone metastases in the mice were monitored weekly through bioluminescent imaging. A week after modeling, 48 animals were randomly divided into the following six groups (n=8): model A group (injection of cancer cells alone, ig saline), model B group (co-injection of cancer cells and BMSCs, ig saline), three dosages of WSZG groups (co-injection of cancer cells and BMSCs, ig 3.25, 6.5, and 13.0 g/kg of WSZG), and zoledronic acid (ZA) group (co-injection of cancer cells and BMSCs, ip 100 μg/kg of ZA solution). The animals were administered WSZG once per day and the ZA solution once per week continuously for four weeks. Additionally, the eight mice used as the normal control group were intracardially injected with saline instead of cancer cells. At the experimental endpoint, all mice were euthanized. Bone fragments were excised, fixed in 4% paraformaldehyde overnight, and stored at -80 °C until further analysis.

In vivo bioluminescent imaging (BLI)

Bioluminescent imaging was performed with an *in vivo* optical imaging system (IVIS 200; Xenogen Corp.) following the procedure of Dragulescu–Andrasi *et al*[12]. All animals were anesthetized with isoflurane gas (2% isoflurane in oxygen, 1 L/min) during the imaging procedure. Each animal was imaged for 8–10 min after intraperitoneal injection of 100 μL of *D*-luciferin solution (15 mg/mL), and a bioluminescence image was then acquired. Signals were quantified with the Living Image software (Xenogen Corp) by drawing a circular ROI around each bioluminescent source. The results are reported as total photon flux within an ROI in photons per second (photons$\cdot s^{-1}\cdot cm^{-2}\cdot sr^{-1}$).

Histology and tartrate-resistant acidic phosphatase (TRAP) staining

Through BLI and radiography, tumor metastatic regions of the spine and limbs were selected from the untreated, WSZG, and ZA-treated groups. Bone fragments were excised, fixed in 4% polyformaldehyde for 48 h, and decalcified in 10% EDTA for 10–14 d. The decalcified bone tissues were embedded in paraffin, sectioned, and stained with hematoxylin and eosin (H&E). TRAP staining was performed using an acid phosphatase kit (Sigma, St Louis, MO, USA) according to the manufacturer's instructions. TRAP-positive osteoclasts existing in trabecular bone surfaces were identified as previously described[13]. Histologic changes were observed, and the number of osteoclasts in 5 consecutive fields of one section per specimen at 40×magnification were counted under a light microscope[14].

Micro-CT imaging

The metastatic lesions of mouse spines were dissected and fixed in 4% paraformaldehyde for 2 h. Then, the samples were scanned by a Quantum FX micro CT Imaging System (PerkinElmer, Inc, USA) at high resolution (36 μm per pixel) using a voltage of 90 kV and a current of 88 μA. Each CT scan was completed in approximately 14 min. Three-dimensional (3D) reconstruction images were acquired by Caliper Analyze and 3D Viewer software (PerkinElmer, Inc, USA).

Immunohistochemistry assay (IHC)

Immunohistochemical staining was performed with a two-step EnVision/HRP system (Dakocytomation, Denmark) according to the manufacturer's instructions. Briefly, decalcified bone sections were blocked with 10% normal goat serum for 30 min and subsequently incubated with primary antibodies to CCL5 (1:100 dilution), CCR5 (1:400 dilution), IL-17B (1:300 dilution), and IL-17BR (1:200 dilution) for 2 h at room temperature. After being washed three times with phosphate-buffered saline, the slides were incubated for 30 min at 37 °C with the EnVision complex (a large number of secondary antibodies and horseradish peroxidase coupled to a dextran backbone). Diaminobenzidine hydrochloride (DAB) was used as the chromogen. The expression of CCL5, CCR5, IL-17B, and IL-17BR was quantitatively evaluated with an Olympus BH2 microscope with a computer-aided image analysis system. The digital images were archived by a digital camera (Nikon 4500, Tokyo, Japan). The positive area and optical density (*OD*) of positive cells were determined by measuring three randomly selected microscopic fields for each slide. The IHC index was defined as the average integral optical density (AIOD) (AIOD=positive area×*OD*/total area).

Real-time quantitative polymerase chain reaction (PCR)

The total RNA of bone tissues was extracted with TRIzol and reverse transcribed to cDNA by using PrimeScript® RT reagent kits according to the manufacturer's instructions. The real-time polymerase chain reaction (PCR)-specific primers were 5′-GGAGTATTTCTACACCAGCAGCAAG-3′ (forward) and 5′-GGCTAGGACTAGAGCAAGCAATGAC-3′ (reverse) for CCL5, 5′-GCAGAAGCTCCAAGAGATGAGGA-3′ (forward) and 5′-A GCCATCTGGAAAGTGTGACTGAA-3′ (reverse) for CCR5, 5′-GAGCCAGCCAAGAAGAAATGTGA-3′(forward) and 5′-GGATTCACGCAACCCAAACATAG-3′ (reverse) for IL-17B, and 5′-GATGGTCCAACACACACTCACTC-3′ (forward) and 5′-GCAGATCTTGGTGGCCTTC-3′ (reverse) for IL-17BR. GAPDH was used as a control to normalize the relative gene expression level. PCR was performed using the following protocol: 95 °C (30 s), 95 °C (5 s), and 60 °C (30 s) in a total of 40 cycles. Real-time PCR was conducted with the ABI Prism 7500 (Applied Biosystems, USA) sequence detection system. The data were analyzed with ABI Step One software version 2.1 (Applied Biosystems, USA). Values are expressed as the cycle threshold (CT) and identified by three indepen-

dent experiments, each of which was performed in triplicate. The fold change in the expression of the detected genes was calculated with the $2^{-\Delta\Delta CT}$ method[15].

Western blotting

Bone tissues were lysed with RIPA buffer containing the protease inhibitor PMSF, and total protein was collected through centrifugation (14 000×*g* for 5 min at 4 °C). The samples (30 μg) were separated with 10%–15% SDS-PAGE gels and transferred onto PVDF membranes (0.45 μm). After blocking with 5% non-fat dry milk, the membranes were incubated with the primary antibodies for CCL5 (1:500), CCR5 (1:100), IL-17B (1:500), IL-17BR (1:100), and β-actin (1:1000) overnight at 4 °C. The membranes were washed three times and incubated with the appropriate HRP-conjugated secondary antibody (1:10000) for 2 h at room temperature. Blots were subsequently visualized using ECL substrates. The images were digitalized with a gel imaging system (Alpha Innotech Corp, USA). β-Actin was used as an internal reference.

Statistics

The data are presented as the mean±SEM. Analysis of variance (ANOVA) was used for multiple comparisons, and Fisher's LSD test or the Games-Howell test was used for the comparison of two mean values. A value of $P<0.05$ was considered statistically significant.

Results

BMSCs promote bone metastasis progression induced by MDA-MB-231BO-Luc breast cancer cells

In vivo bioluminescent imaging was performed after intracardiac injection of MDA-MB-231BO-Luc cells alone (model A group) or MDA-MB-231BO-Luc+BMSCs (model B group) into nude mice. Representative bioluminescent images of bone metastasis progression are shown in Figure 1. One week after injection, bioluminescent signals indicating bone metastases began to appear at a few sites in the two groups. After 3–4 weeks, the mice exhibited evident bioluminescent signals of bone metastases at multiple sites in the head, spine, and limbs. After five weeks, the intensity of the bioluminescent signals reached the maximum level. The bioluminescent intensities in the model B group were significantly higher than those in the model A group.

Effect of WSZG on the incidence and intensity of bone metastasis induced by MDA-MB-231BO+BMSC co-injection in nude mice

Four weeks after treatment with drugs or saline, the bioluminescent signals in each group were detected and quantified by *in vivo* BLI. As shown in Figure 2A, the BLI signals in WSZG and ZA-treated groups were relatively weaker than those in the two model groups. Similar to the BLI observation, treatment with WSZG and ZA significantly reduced the total tumor burden, which was determined by the radiance of tumor luminescence compared with the model B group ($P<0.05$ or $P<0.01$, Figure 2B). Furthermore, the model B group exhibited a higher frequency of bone metastases than the model A group. WSZG and ZA significantly reduced the number of bone metastatic sites ($P<0.05$ or $P<0.01$, Figure 2C).

Effect of WSZG on metastatic bone lesions induced by MDA-MB-231BO+BMSC co-injection in nude mice

As shown in the 3D micro-CT scanning image of tumor-bearing spines in different groups, MDA-MB-231BO breast cancer cells clearly caused osteolytic bone lesions, and BMSCs further aggravated the severity of bone erosion. Treatment with WSZG or ZA markedly reduced the extent of bone lesions

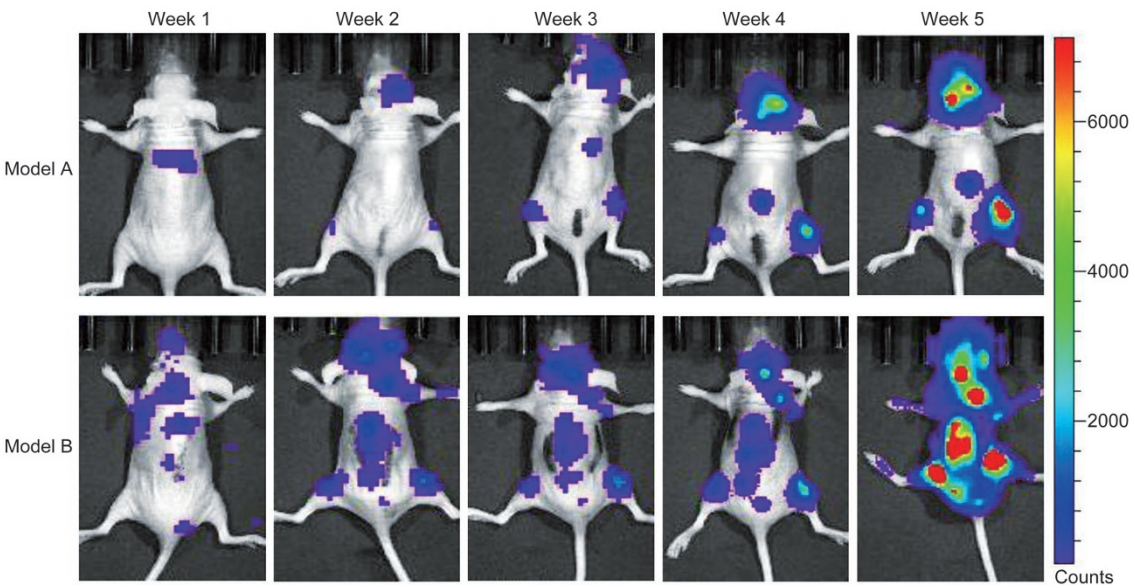

Figure 1. Representative bioluminescent images of bone metastasis progression from model A and model B groups at week 1, 2, 3, 4, and 5 after intracardiac injection of MDA-MB-231BO-Luc breast cancer cells alone or mixture with BMSCs. BLI signals revealed that BMSCs induced higher frequency of MDA-MB-231BO breast cancer cell metastasis to skeleton. BMSCs: bone marrow-derived stem cells; BLI: bioluminescent imaging.

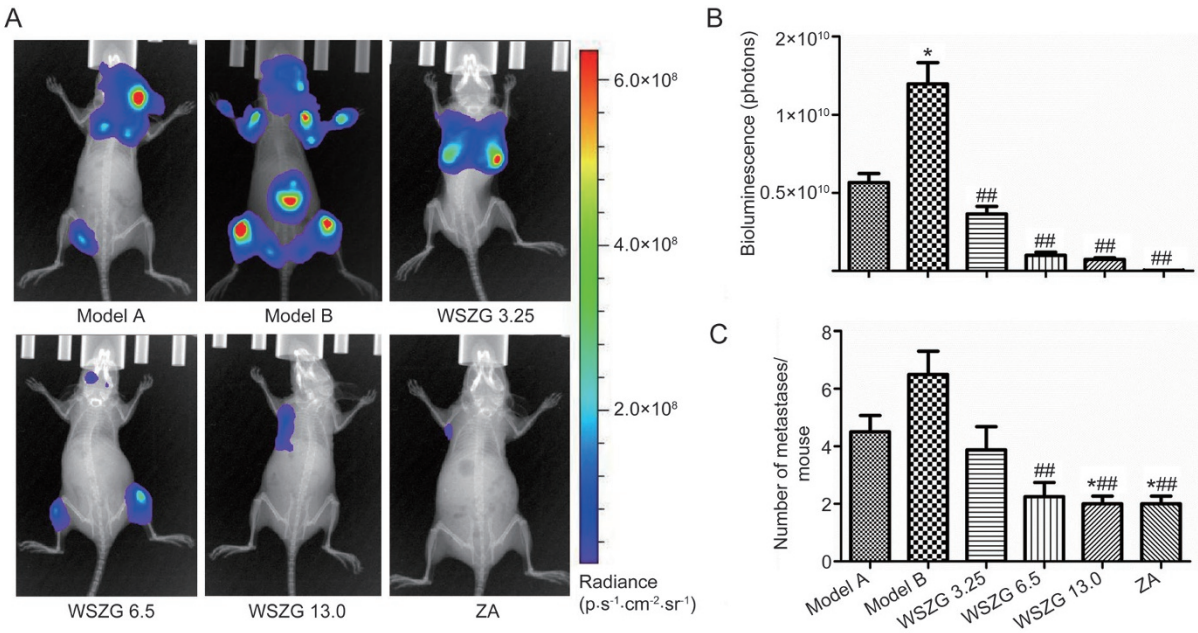

Figure 2. Effect of WSZG treatment on the incidence and intensity of bone metastasis in nude mice assessed by bioluminescent imaging. (A) Representative bioluminescent images of untreated groups (model A and model B), WSZG-treated groups (ig 3.25, 6.5, and 13.0 g·kg^{-1}·d^{-1}), and ZA-treated group (ip 100 μg/kg) taken at week 5 after intracardiac injection of MDA-MB-231BO-Luc breast cancer cells alone or mixture with BMSC. (B) The total tumor burden measured by radiance of luminescence per group. (C) The average number of bone metastases per group. Data are expressed as mean±SEM (n=8). $^{*}P$<0.05 *vs* model A group. $^{\#\#}P$<0.01 *vs* model B group. WSZG: Wenshen Zhuanggu formula; ZA: zoledronic acid; BMSCs: bone marrow-derived stem cells.

when compared to the model groups (Figure 3A). H&E staining revealed extensive tumor cell infiltrations and partial bone destruction in bone metastatic tissues from the model mice. By contrast, treatment with WSZG or ZA distinctly alleviated the extent of tumor cell infiltrations in bone tissues (Figure 3B). To confirm the effect of WSZG on the number of osteoclasts, spine sections were stained with TRAP. As shown in Figure 3C, TRAP-positive multinucleated cells located at the trabecular bone surface were considered osteoclasts. Compared to normal mice, model mice had a significantly higher number of osteoclasts in the region with metastatic bone lesions (P<0.01). WSZG (6.5, and 13.0 g·kg^{-1}·d^{-1}) and ZA treatment effectively decreased the number of osteoclasts in the region with metastatic bone lesions compared to model groups (P<0.05 or P<0.01). Additionally, there was no difference in the number of osteoclasts between model A and model B groups (P>0.05).

Effect of WSZG on CCL5/CCR5 and IL-17B/IL-17BR mRNA expression in bone metastatic tissues

Growing evidence demonstrates that the CCL5/CCR5 and IL-17B/IL-17BR axis may be linked to breast cancer progression induced by the interaction between BMSCs and breast cancer cells[16–19]. Thus, we further investigated the effect of WSZG on the gene expression levels of bone metastatic tissues from a breast cancer xenograft model. Real-time PCR analysis showed that the expression levels of the four genes in bone metastatic tissues from model B mice were overexpressed greater than 12–20-fold in bone metastatic tissues from normal mice. By contrast, different doses of WSZG-treated mice exhibited a 3.4–5.1-fold, 1.0–3.0-fold, 1.4–5.6-fold, and 4.1–9.2-fold downregulation in CCL5, CCR5, IL-17B, and IL-17BR mRNA levels, respectively. Compared with the model B group, WSZG and ZA significantly inhibited the expression of these genes (Figure 4, P<0.05 or P<0.01).

Effect of WSZG on CCL5/CCR5 and IL-17B/IL-17BR protein expression in bone metastatic tissues

Immunohistochemical assay

As shown in Figure 5, the protein levels of CCL5/CCR5 and IL-17B/IL-17BR were significantly overexpressed in breast cancer bone metastatic regions relative to those in normal bone tissues. Furthermore, co-injection of MDA-MB-231BO cancer cells with BMSCs slightly increased the expression of the four proteins compared with the injection of MDA-MB-231BO cells alone. After treatment with WSZG and ZA, these proteins expression decreased steadily. Consistent with the IHC stain, the IHC indexes of CCL5/CCR5 and IL-17B/IL-17BR in the model A and model B groups were considerably higher than those in the normal group (P<0.05 or P<0.01). Compared with the model B group, the IHC index of all proteins significantly decreased in the WSZG (6.50 and 13.0 g/kg) and ZA groups (P<0.05 or P<0.01). The IHC index of CCL5 and IL-17B was also significantly reversed in the WSZG group (3.25 g/kg; P<0.01). In addition, significant differences were observed in the IHC indexes of CCR5 and IL-17B between the WSZG-treated groups and the model A group (P<0.01).

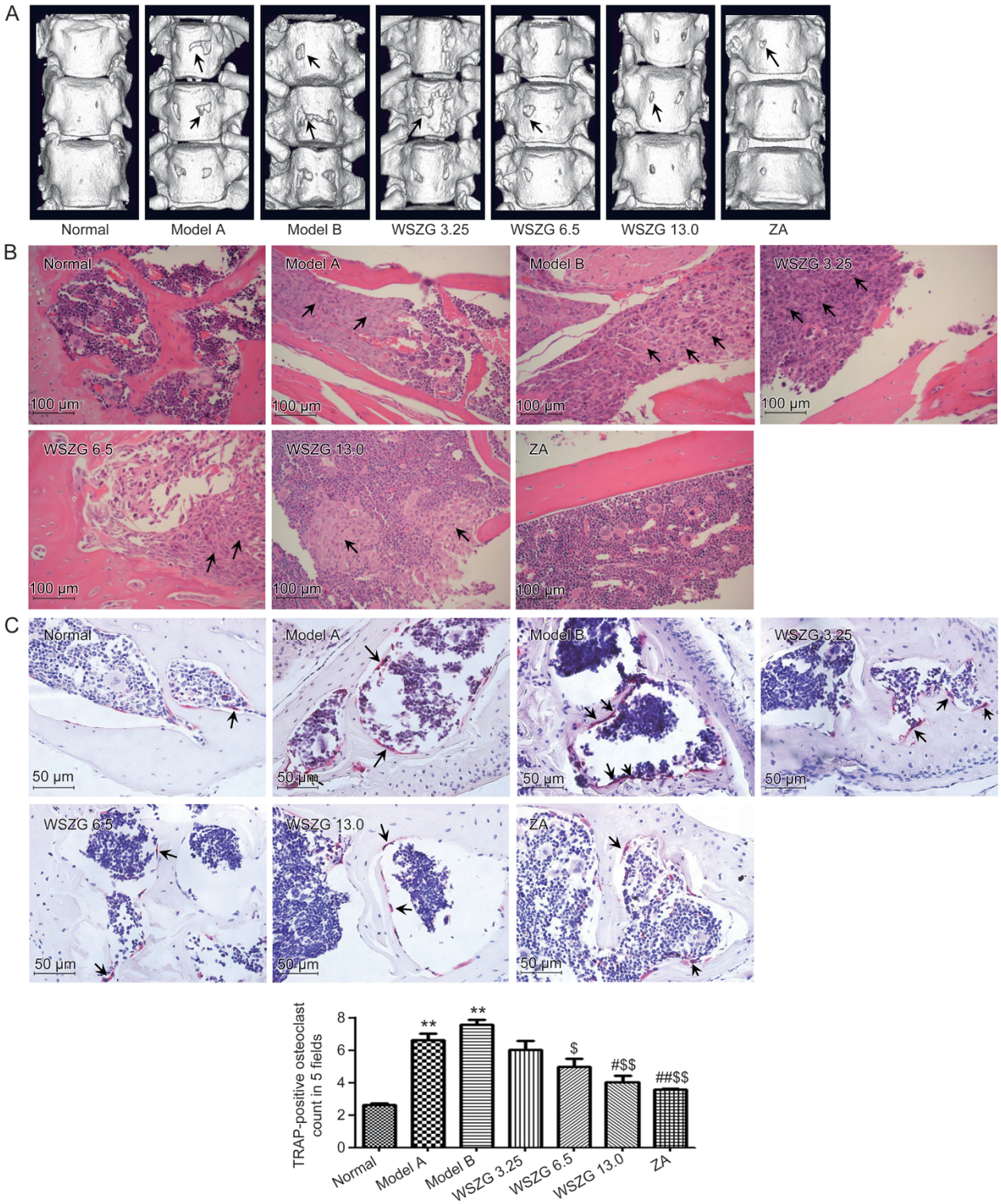

Figure 3. Effect of WSZG treatment on metastatic bone lesions caused by co-injection of MDA-MB-231BO cells with BMSCs. One week after intracardiac injection of breast cancer cells alone or mixture with BMSCs, the nude mice were administered WSZG (ig 3.25, 6.5, and 13.0 g·kg^{-1}·d^{-1}), ZA (ip 100 μg/kg) or saline for 4 weeks. (A) The typical images of three-dimensional reconstructed spinal bones *via* micro-CT scanning in different groups (black arrowheads note bone lesion areas). (B) The representative H&E staining of tibial sections in different groups (black arrowheads note tumor cell infiltration in bone tissues, 20×objective, scale bar is 100 μm). (C) The representative TRAP-stained histological spinal sections in different groups (black arrowheads note osteoclasts, 40×objective, and scale bar is 50 μm). The number of TRAP-positive osteoclasts from the bone lesion areas in 5 consecutive fields at one section per specimen was counted under light microscope (n=6, mean±SEM). $^{**}P$<0.01 *vs* normal group; $^{\#}P$<0.05, $^{\#\#}P$<0.01 *vs* model A group; $^{\$}P$<0.05, $^{\$\$}P$<0.01 *vs* model B group. WSZG: Wenshen Zhuanggu formula; ZA: zoledronic acid; BMSCs: bone marrow-derived stem cells; H&E: hematoxylin and eosin; TRAP: tartrate-resistant acidic phosphatase.

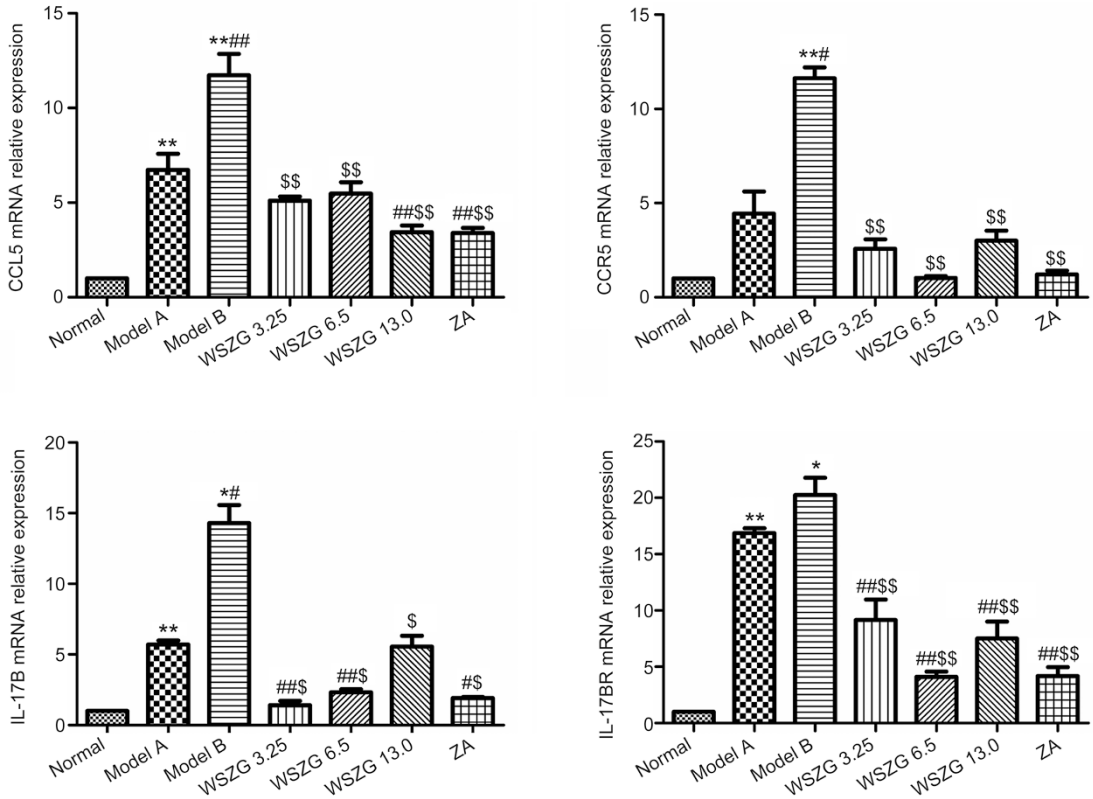

Figure 4. Effect of WSZG on the mRNA levels of CCL5/CCR5 and IL-17B/IL-17BR in bone metastatic tissues induced by co-injection of MDA-MB-231BO cells with BMSCs. After treatment with (ig 3.25, 6.5, and 13.0 g·kg^{-1}·d^{-1}) or ZA (ip 100 μg/kg) for 4 weeks, the relative expression of CCL5, CCR5, IL-17B, and IL-17BR mRNA were determined by real-time PCR (n=3, mean±SEM). Each experiment was performed three times. $^{*}P$<0.05, $^{**}P$<0.01 *vs* normal group; $^{\#}P$<0.05, $^{\#\#}P$<0.01 *vs* model A group; $^{\$}P$<0.05, $^{\$\$}P$<0.01 *vs* model B group. WSZG: Wenshen Zhuanggu formula; ZA: zoledronic acid; BMSCs: bone marrow-derived stem cells.

Western blotting analysis

We further investigated the protein expression levels of CCL5/CCR5 and IL-17B/IL-17BR associated with the interaction between BMSCs and breast cancer cells in bone metastatic tissues through Western blotting. Consistent with the results of the IHC assay, a remarkable increase in the four proteins levels was observed in the bone metastasis tissues from model B mice (Figure 6A; P<0.01 *vs* normal mice). Compared to the model B group, WSZG (6.50 and 13.0 g/kg) treatment significantly inhibited the expression levels of the four proteins in bone metastasis tissues. The protein inhibition was 42.3%–43.1% in CCL5, 46.8%–58.2% in CCR5, 73.8%–77.3% in IL-17B, and 44.2%–52.7% in IL-17BR proteins (Figure 6B; P<0.05 or P<0.01). Similarly, ZA also significantly suppressed the expression of these proteins (P<0.01).

Discussion

It has been reported that human BMSCs play a fundamental role in breast cancer pathogenesis[20–22]. BMSCs are recruited to the stroma of the primary tumor site, where they might facilitate breast cancer cell invasion and distant metastasis[23]. Our previous data have shown that WSZG exerted an inhibitory effect on BMSC-induced MDA-MB-231BO breast cancer cell migration *in vitro*[10]. However, the anti-metastatic efficacy of WSZG *in vivo* is unclear. In the current study, we further investigated the potential effect of this formula on a mouse model of bone metastasis mediated by the interaction between BMSCs and breast cancer cells (BCCs).

In our xenograft model, bioluminescent signals were clearly visible in the skeleton five weeks after the initial injection of tumor cells. Bone lesions were further confirmed by micro-CT and histological analysis. The results showed that MDA-MB-231BO BCCs co-injected with BMSCs at a ratio of 1:1 caused a much higher frequency of bone metastasis and tumor burden compared to BCCs injected alone. However, WSZG treatment (6.5 and 13.0 g/kg) for 4 weeks significantly reduced the incidence and intensity of BCC metastasis in the co-injection model. Importantly, WSZG could also effectively prevent bone lesions by suppressing osteoclast formation and tumor cell infiltration. In addition, we have previously reported a significant decrease in the number of bone metastatic sites and in the extent of bone destruction following administration of WSZG (7.5 and 15 g/kg) in the mono-injection model[6]. Therefore, it has been postulated that WSZG might directly act on BCCs to inhibit metastasis to bone, or indirectly *via* weakening the interaction of cancer cells with BMSCs.

In multiple studies, the chemokine C–C motif ligand 5 (CCL5) and chemokine receptor (CCR5) axis has been indi-

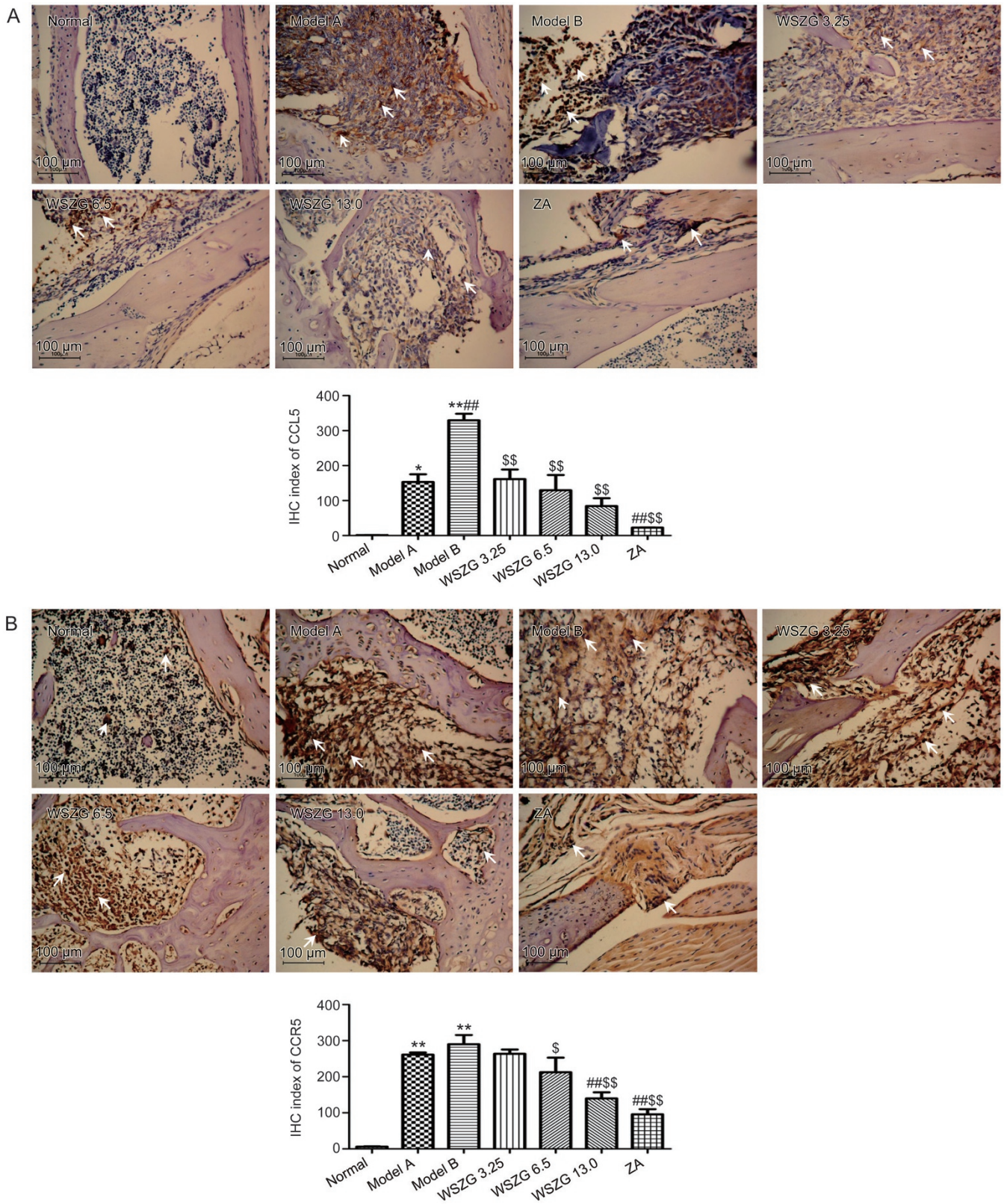

Figure 5A, 5B. Immunohistochemical (IHC) analysis of CCL5 (A)/CCR5 (B) protein expression in bone metastatic tissues following treatment with saline, WSZG (ig 3.25, 6.5, and 13.0 g·kg^{-1}·d^{-1}) or ZA (ip 100 μg/kg). Representative images of IHC staining are shown (original magnification ×200), white arrowheads note the immunoreactive cells in different groups and scale bar is 100 μm. IHC index are calculated by measuring three randomly selected microscopic fields for each slide (n=5, mean±SEM). $^{*}P$<0.05, $^{**}P$<0.01 *vs* normal group; $^{\#}P$<0.05, $^{\#\#}P$<0.01 *vs* model A group; $^{\$}P$<0.05, $^{\$\$}P$<0.01 *vs* model B group. WSZG: Wenshen Zhuanggu formula; ZA: zoledronic acid.

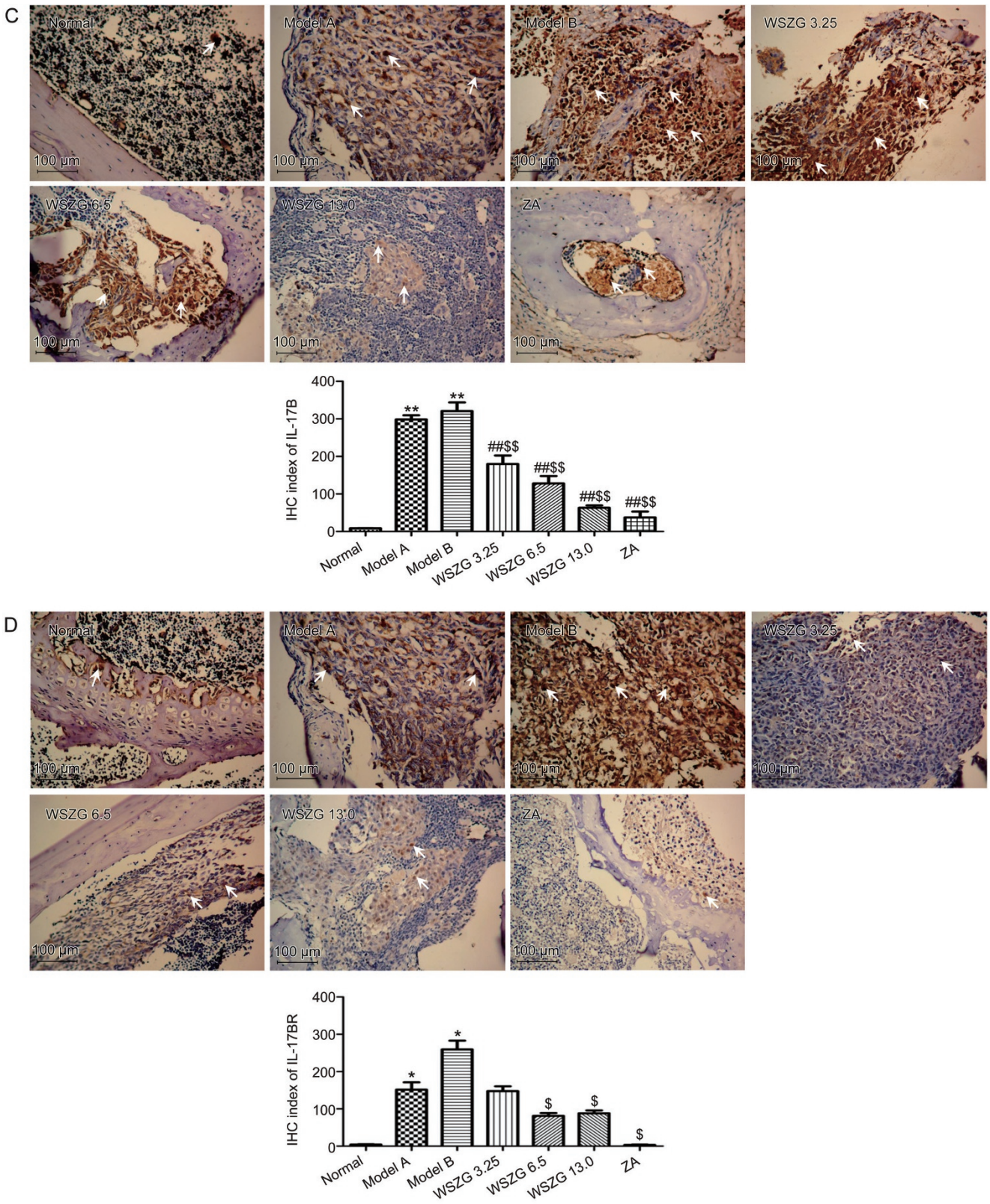

Figure 5C, 5D. Immunohistochemical (IHC) analysis of IL-17B (C)/IL-17BR (D) protein expression in bone metastatic tissues following treatment with saline, WSZG (ig 3.25, 6.5, and 13.0 $g{\cdot}kg^{-1}{\cdot}d^{-1}$) or ZA (ip 100 μg/kg). Representative images of IHC staining are shown (original magnification ×200), white arrowheads note the immunoreactive cells in different groups and scale bar is 100 μm. IHC index are calculated by measuring three randomly selected microscopic fields for each slide (n=5, mean±SEM). $^{*}P$<0.05, $^{**}P$<0.01 *vs* normal group; $^{\#}P$<0.05, $^{\#\#}P$<0.01 *vs* model A group; $^{\$}P$<0.05, $^{\$\$}P$<0.01 *vs* model B group. WSZG: Wenshen Zhuanggu formula; ZA: zoledronic acid.

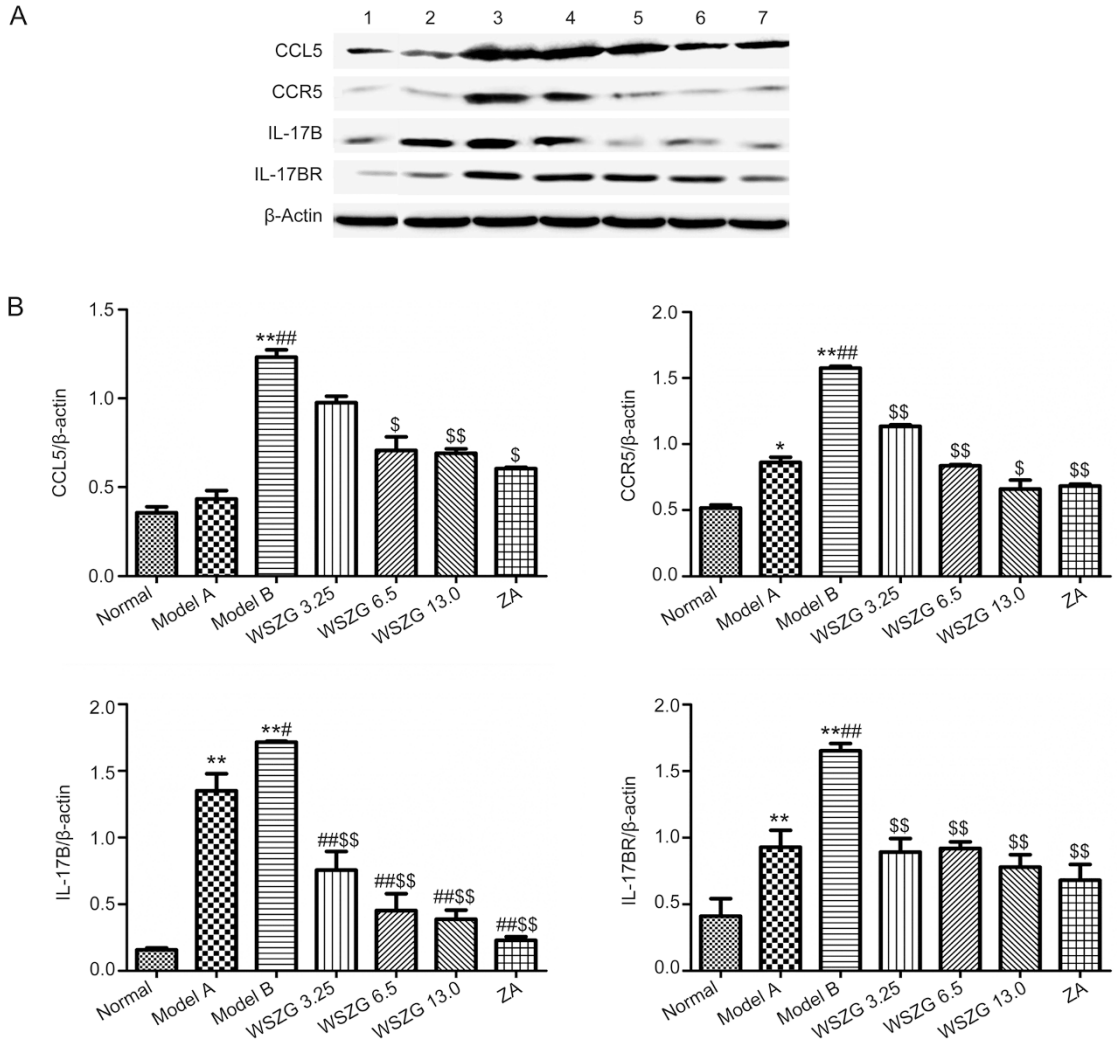

Figure 6. Effects of WSZG treatment on CCL5/CCR5 and IL-17B/IL-17BR signaling proteins in bone metastatic tissues induced by co-injection of MDA-MB-231BO cells with BMSCs. (A) Changes in protein expression of CCL5/CCR5 and IL-17B/IL-17BR were determined by Western blotting analysis in different groups. β-Actin was used as an internal loading control. 1: normal; 2: model A; 3: model B; 4–6: WSZG (3.25, 6.5, and 13.0 g·kg^{-1}·d^{-1}); 7: ZA 100 μg/kg. (B) Relative quantities of Western blotting are shown by bar graph (n=3, mean±SEM). $^{*}P$<0.05, $^{**}P$<0.01 *vs* normal group; $^{\#}P$<0.05, $^{\#\#}P$<0.01 *vs* model A group; $^{\$}P$<0.05, $^{\$\$}P$<0.01 *vs* model B group. WSZG: Wenshen Zhuanggu formula; ZA: zoledronic acid. BMSCs: bone marrow-derived mesenchymal stem cells.

cated to facilitate breast cancer progression and metastasis by mediating the interaction of BMSCs with tumor cells[24, 25]. CCL5 is not only highly expressed by BCCs at the primary tumor and metastatic sites[26, 27] but also expressed by stromal and immune cells, such as BMSCs, tumor-associated macrophages[28], myeloid-derived suppressor cells, and T-regulatory cells[29], in the tumor microenvironment. BCCs stimulate CCL5 secretion by BMSCs or other cells, and then CCL5 acts by binding with the highest affinity to CCR5 in BCCs to enhance their motility, invasion, and metastasis to distant organs[24, 30]. The potential mechanisms for these actions include promoting the recruitment of additional stromal cells, participating in the immune response, activating matrix metalloproteinase, *etc*[31].

Additionally, recent studies have reported that interleukin 17 (IL-17) family members and their receptors are closely correlated to tumor malignancy and progression[32–34]. As a pro-inflammatory cytokine, IL-17B is mainly produced by helper T (Th) 17 cells, innate and adaptive immune cells, and BMSCs[35–38], and its receptor (IL-17BR) is present on tumor cells. Activated IL-17B/IL-17BR signaling can increase the tumorigenic and metastatic abilities of tumor cells *via* stimulating the secretion of chemokines or enhancing inflammatory activities[34, 39]. Notably, a previous study also found that IL-17B/IL-17BR signaling could promote bone metastasis by mediating the interaction of BMSCs with BCCs[3]. Taken together, CCL5/CCR5 and IL-17B/IL-17BR may represent important biomarkers and therapeutic targets for breast cancer progression.

Therefore, we further assessed whether the anti-metastatic effect of WSZG was indirectly dependent on the interaction

between BCCs and BMSCs mediated by the CCL5/CCR5 and IL-17B/IL-17BR signals *in vivo*. Our data showed that the mRNA and proteins of CCL5/CCR5 and IL-17B/IL-17BR were significantly overexpressed in bone metastases following co-injection of BMSCs with MDA-MB-231BO cells when compared to normal bone tissues. Conversely, four-week treatment with WSZG at different doses substantially downregulated the expression of these signaling molecules in bone metastatic tissues. Similarly, we have previously found that WSZG reduced BMSC-secreted CCL5 and IL-17B levels and decreased CCR5 and IL-17BR protein expression in BCCs *in vitro*[10]. The inhibition of the metastatic ability of MDA-MB-231BO cells by WSZG treatment, at least partially, was dependent on the CCL5/CCR5 and IL-17B/IL-17BR axis.

In summary, WSZG treatment efficiently reduced the risk of bone metastases and the bone lesions in a mouse xenograft model of breast cancer. Its therapeutic effect was partially achieved by impairing the interaction of BMSCs with BCCs in the tumor microenvironment. Therefore, our findings suggest that WSZG may serve as a potential anti-metastatic agent for breast cancer. The cross-talk between BMSCs and tumor cells mediated by different signaling pathways also needs further exploration in the future.

Acknowledgements

This work was supported by the National Natural Science Foundation of China (No 81102598, 81573973, 81603629) and the Program for Longhua Medical Research Team (No LYTD-17).

Author contribution

Jia-jia LI and Wei-ling CHEN conducted the main experiments and data analyses; Qian-wen HU carried out the animal study and wrote the manuscript; Jian-yi WANG conducted the quality control of the extract; Zhen-ping SUN and Shuai ZHANG conducted the pathological and immunohistochemical analysis; Sheng LIU provided guidance during the experiments; and Xiang-hui HAN designed the study and revised the manuscript. All authors approved the final manuscript.

References

1 Weil RJ, Palmieri DC, Bronder JL, Stark AM, Steeg PS. Breast cancer metastasis to the central nervous system. Am J Pathol 2005; 167: 913–20.
2 Scully OJ, Bay BH, Yip G, Yu Y. Breast cancer metastasis. Cancer Genomics Proteomics 2012; 9: 311–20.
3 Goldstein RH, Reagan MR, Anderson K, Kaplan DL, Rosenblatt M. Human bone marrow-derived MSCs can home to orthotopic breast cancer tumors and promote bone metastasis. Cancer Res 2010; 70: 10044–50.
4 Zhu L, Li L, Li Y, Wang J, Wang Q. Chinese herbal medicine as an adjunctive therapy for breast cancer: a systematic review and meta-analysis. Evid Based Complement Alternat Med 2016; 2016: 9469276.
5 Sun ZP. Professor LU De-ming's clinical experiences and observations on the treatment of breast cancer bone metastasis [dissertation]. Shanghai (China): Shanghai TCM Univ; 2010.
6 Zhang XH, Han XH, Liu S, Guo BF, Wang CL. Effect of WSZG recipe on Tac1/NK1R signaling pathway proteins in nude mice with bone metastasis in breast cancer. Chin Trad Patent Med 2014; 36: 1569–73. Chinese.
7 Pittenger MF, Mackay AM, Beck SC, Jaiswal RK, Douglas R, Mosca JD, *et al*. Multilineage potential of adult human mesenchymal stem cells. Science 1999; 284: 143–7.
8 Meleshina AV, Cherkasova EI, Shirmanova MV, Klementieva NV, Kiseleva EV, Snopova LB, *et al*. Influence of mesenchymal stem cells on metastasis development in mice *in vivo*. Stem Cell Res Ther 2015; 6: 15.
9 Suva LJ, Griffin RJ, Makhoul I. Mechanisms of bone metastases of breast cancer. Endocr Relat Cancer 2009; 16: 703–13.
10 Han XH, Wang CL, Xie Y, Ma J, Zhang XH, Hu QW, *et al*. Anti-metastatic effect and mechanisms of Wenshen Zhuanggu Formula in human breast cancer cells. J Ethnopharmacol 2015; 162: 39–46.
11 Yoneda T, Williams PJ, Hiraga T, Niewolna M, Nishimura R. A bone-seeking clone exhibits different biological properties from the MDA-MB-231 parental human breast cancer cells and a brain seeking clone *in vivo* and *in vitro*. J Bone Miner Res 2001; 16: 1486–95.
12 Dragulescu-Andrasi A, Liang G, Rao J. *In vivo* bioluminescence imaging of furin activity in breast cancer cells using bioluminogenic substrates. Bioconjug Chem 2009; 20: 1660–6.
13 Park BK, Zhang H, Zeng Q, Dai J, Keller ET, Giordano T, *et al*. NF-kappaB in breast cancer cells promotes osteolytic bone metastasis by inducing osteoclastogenesis via GM-CSF. Nat Med 2007; 13: 62–9.
14 Tu Q, Zhang J, Fix A, Brewer E, Li YP, Zhang ZY, *et al*. Targeted overexpression of BSP in osteoclasts promotes bone metastasis of breast cancer cells. J Cell Physiol 2009; 218: 135–45.
15 Livak KJ, Schmittgen TD. Analysis of relative gene expression data using real-time quantitative PCR and the $2^{-\Delta\Delta CT}$ method. Methods 2001; 25: 402–8.
16 Jung MY, Kim SH, Cho D, Kim TS. Analysis of the expression profiles of cytokines and cytokine-related genes during the progression of breast cancer growth in mice. Oncol Rep 2009; 22: 1141–7.
17 Dunn L, Demichele A. Genomic predictors of outcome and treatment response in breast cancer. Mol Diagn Ther 2009; 13: 73–90.
18 Huang H, Kim HJ, Chang EJ, Lee ZH, Hwang SJ, Kim HM, *et al*. IL-17 stimulates the proliferation and differentiation of human mesenchymal stem cells: implications for bone remodeling. Cell Death Differ 2009; 16: 1332–43.
19 Cambien B, Richard-Fiardo P, Karimdjee BF, Martini V, Ferrua B, Pitard B, *et al*. CCL5 neutralization restricts cancer growth and potentiates the targeting of PDGFRβ in colorectal carcinoma. PLoS One 2011; 6: e28842.
20 Li M, Cai H, Yang Y, Zhang J, Sun K, Yan Y, *et al*. Perichondrium mesenchymal stem cells inhibit the growth of breast cancer cells via the DKK-1/Wnt/β-catenin signaling pathway. Oncol Rep 2016; 36: 936–44.
21 Yang X, Hao J, Mao Y, Jin ZQ, Cao R, Zhu CH, *et al*. bFGF promotes migration and induces cancer-associated fibroblast differentiation of mouse bone mesenchymal stem cells to promote tumor growth. Stem Cells Dev Epub 2016 Sep 12. Doi: 10.1089/scd.2016.0217.
22 Chiovaro F, Martina E, Bottos A, Scherberich A, Hynes NE, Chiquet-Ehrismann R. Transcriptional regulation of tenascin-W by TGF-beta signaling in the bone metastatic niche of breast cancer cells. Int J Cancer 2015; 137: 1842–54.
23 Normanno N, De Luca A, Aldinucci D, Maiello MR, Mancino M, D'Antonio A, *et al*. Gefitinib inhibits the ability of human bone marrow stromal cells to induce osteoclast differentiation: implications for the pathogenesis and treatment of bone metastasis. Endocr Relat

Cancer 2005; 12: 471–82.
24 Karnoub AE, Dash AB, Vo AP, Sullivan A, Brooks MW, Bell GW, *et al*. Mesenchymal stem cells within tumour stroma promote breast cancer metastasis. Nature 2007; 449: 557–63.
25 Mi Z, Bhattacharya SD, Kim VM, Guo H, Talbot LJ, Kuo PC. Osteopontin promotes CCL5-mesenchymal stromal cell-mediated breast cancer metastasis. Carcinogenesis 2011; 32: 477–87.
26 Zhang Y, Liao S, Fan W, Wei W, Wang C, Sun S. Tunicamycin-induced ER stress regulates chemokine CCL5 expression and secretion via STAT3 followed by decreased transmigration of MCF-7 breast cancer cells. Oncol Rep 2014; 32: 2769–76.
27 Swamydas M, Ricci K, Rego SL, Dreau D. Mesenchymal stem cell-derived CCL-9 and CCL-5 promote mammary tumor cell invasion and the activation of matrix metalloproteinases. Cell Adh Migr 2013; 7: 315–24.
28 Cook J, Hagemann T. Tumour-associated macrophages and cancer. Curr Opin Pharmacol 2013; 13: 595–601.
29 Chang LY, Lin YC, Mahalingam J, Huang CT, Chen TW, Kang CW, *et al*. Tumor-derived chemokine CCL5 enhances TGF-beta-mediated killing of CD8(+) T cells in colon cancer by T-regulatory cells. Cancer Res 2012; 72: 1092–102.
30 Zhang Y, Yao F, Yao X, Yi C, Tan C, Wei L, *et al*. Role of CCL5 in invasion, proliferation and proportion of $CD44^+/CD24^-$ phenotype of MCF-7 cells and correlation of CCL5 and CCR5 expression with breast cancer progression. Oncol Rep 2009; 21: 1113–21.
31 Kershaw MH, Westwood JA, Darcy PK. Gene-engineered T cells for cancer therapy. Nat Rev Cancer 2013; 13: 525–41.
32 Furuta S, Jeng YM, Zhou L, Huang L, Kuhn I, Bissell MJ, *et al*. IL-25 causes apoptosis of IL-25R-expressing breast cancer cells without toxicity to nonmalignant cells. Sci Transl Med 2011; 3: 78ra31.
33 Huang CK, Yang CY, Jeng YM, Chen CL, Wu HH, Chang YC, *et al*. Autocrine/paracrine mechanism of interleukin-17B receptor promotes breast tumorigenesis through NF-kappaB-mediated antiapoptotic pathway. Oncogene 2014; 33: 2968–77.
34 Wu HH, Hwang-Verslues WW, Lee WH, Huang CK, Wei PC, Chen CL, *et al*. Targeting IL-17B-IL-17RB signaling with an anti-IL-17RB antibody blocks pancreatic cancer metastasis by silencing multiple chemokines. J Exp Med 2015; 212: 333–49.
35 Cua DJ, Tato CM. Innate IL-17-producing cells: the sentinels of the immune system. Nat Rev Immunol 2010; 10: 479–89.
36 Huber M, Heink S, Pagenstecher A, Reinhard K, Ritter J, Visekruna A, *et al*. IL-17A secretion by $CD8^+$ T cells supports Th17-mediated autoimmune encephalomyelitis. J Clin Invest 2013; 123: 247–60.
37 Bermejo DA, Jackson SW, Gorosito-Serran M, Acosta-Rodriguez EV, Amezcua-Vesely MC, Sather BD, *et al*. Trypanosoma cruzi trans-sialidase initiates a program independent of the transcription factors RORgammat and Ahr that leads to IL-17 production by activated B cells. Nat Immunol 2013; 14: 514–22.
38 Yang R, Liu Y, Kelk P, Qu C, Akiyama K, Chen C, *et al*. A subset of IL-17(+) mesenchymal stem cells possesses anti-*Candida albicans* effect. Cell Res 2013; 23: 107–21.
39 Lee WH, Wu HH, Huang CK. Targeting interleukin-17 receptors. Oncotarget 2015; 6: 18244–5.